

An elastic two-sphere swimmer in Stokes flow

Babak Nasouri, Aditi Khot, and Gwynn J. Elfring*

Department of Mechanical Engineering, University of British Columbia, Vancouver, B.C., V6T 1Z4, Canada

Swimming at low Reynolds number in Newtonian fluids is only possible through non-reciprocal body deformations due to the kinematic reversibility of the Stokes equations. We consider here a model swimmer consisting of two linked spheres, wherein one sphere is rigid and the other an incompressible neo-Hookean solid. The two spheres are connected by a rod which changes its length periodically. We show that the deformations of the body are non-reciprocal despite the reversible actuation and hence, the elastic two-sphere swimmer propels forward. Our results indicate that even weak elastic deformations of a body can qualitatively alter swimming dynamics and should not be neglected in analyzing swimming in Stokes flows.

1. INTRODUCTION

In the microscale realm of motile cells, inertia is unimportant and the effect of viscous dissipation dominates the fluid forces on swimming bodies [1, 2]. To propel forward in this regime, many microorganisms deform their bodies periodically by converting cells' chemical energy into mechanical work [3]. As a direct consequence of this inertialess environment, to achieve nonzero net locomotion, such body deformations cannot be invariant under time reversal [4]. This constraint, colloquially referred to as the scallop theorem, indicates that due to the kinematic reversibility of the field equations in the low Reynolds number regime, reciprocal body distortions have no net effect.

Theoretically, the scallop theorem can be eluded under two circumstances: non-reciprocal kinematics or a violation of the theorem's assumptions (see [5] and the references therein). The latter exploits the fact that the scallop theorem is solely valid for inertialess single swimmers in quiescent viscous fluid. Therefore, hydrodynamic interactions [6], a non-Newtonian medium [7], or inertia [8] can all lead to propulsion. Non-reciprocal kinematics is the primary swimming technique of the most of motile cells [9, 10]. This technique, which for rigid bodies requires at least two degrees of freedom, has become the core concept behind model swimmers at small scales. In 1977, Purcell introduced a simple three-link swimmer with two rotational hinges that can change its shape in a non-reciprocal fashion, leading to a locomotion [4]. Subsequently, several analytical model swimmers have been devised wherein shape change provides the propulsive thrust [11–14]. Notably, Najafi and Golestanian [15] proposed a simple three-sphere swimmer, in which spheres are identical and connected by two slender rods. The connecting rods change their length in a four-stage cycle that is not invariant under time reversal. After completion of one cycle, the swimmer recovers its original shape but has been translated forward (see also [16] and [17]). Avron *et al.* [18] suggested a more efficient, yet as simple, swimmer that consists of two linked spherical bladders of different radii. To compensate for the third sphere, they relaxed the rigidity constraint by allowing instantaneous volume exchange between spherical bladders in each stroke. The shape change of the bladders along with the periodic change in their distance, leads to a net displacement of the swimmer. Inspired by these two models, in this paper we investigate a simple, but more intuitive, two-sphere swimmer where one of the spheres is elastic. We propose that the elasticity of the swimmer is sufficient to escape the scallop theorem, alter the hydrodynamic interactions and eventually lead to propulsion.

Elasticity, as an inevitable characteristic of motile cells, can significantly affect the hydrodynamics of a motion. The propulsion of flexible bodies [4, 19, 20], synchronization of flagella [21, 22], and cilia [23–25], through elastohydrodynamic interactions and reorientation of uni-flagellated bacteria due to buckling of the flagellum [26, 27] are well-studied examples of such behaviors. For an elastic body in a flow, the balance of viscous forces, external forces and internal elastic forces causes the body to deform and to alter the surrounding flow field, often in a complex fashion [28–30]. Li *et al.* [28] reported that for an isolated sedimenting filament, elasticity can destabilize the motion and lead to a substantial buckling. Furthermore, Gao *et al.* [29] showed that elastic spheres in a shear flow exhibit a 'tank-treading' motion wherein the particle shape is at steady state while the material points on the boundary are undergoing a periodic motion. However, though seemingly simple, sedimentation of spherical elastic particles in a viscous fluid is largely unexplored. The most recent, and to the best of our knowledge the only, analysis on sedimentation of elastic spheres dates back to more than three decades ago, when Murata [31] investigated the steady state shape deformation of a compressible, Hookean sphere. Using an asymptotic analysis, it was shown that the elastic sphere settles faster and deforms to a prolate spheroid of a smaller volume. In this work, to further investigate the deformation of

* Electronic mail: gelfring@mech.ubc.ca

elastic spheres, we revisit this sedimentation problem but this time for an incompressible neo-Hookean sphere under a prescribed body force. We asymptotically describe the steady state effects of non-linear elastic deformations on the swimming behaviors of an isolated elastic sphere.

The paper is organized as follows. In section 2, we investigate the translation of a single neo-Hookean sphere in Stokes flow. Using an asymptotic approach, we show that for a given body force, due to shape deformation, the translational velocity of the elastic sphere is smaller compared to a rigid sphere of the same size. Furthermore, we find that the shape deformation is not front-back symmetric and so neither is the flow field generated in the surrounding fluid. In section 3, we show that by exploiting this asymmetry, the proposed two-sphere model can indeed swim in a low Reynolds number regime. Finally, in the case where the distance between the spheres is relatively large, we determine the propulsion velocity.

2. TRANSLATION OF AN ELASTIC SPHERE

We begin our analysis with considering the translation of an incompressible isotropic neo-Hookean sphere in an otherwise quiescent viscous fluid. The sphere has radius R_0 and is driven by body force $\mathbf{f}(t)$. In the fluid domain (Ω_f) , the flow field around the sphere is governed by the Stokes equations

$$\nabla \cdot \boldsymbol{\sigma}_f = \mathbf{0}, \quad (2.1)$$

$$\nabla \cdot \mathbf{v} = 0, \quad (2.2)$$

where \mathbf{v} is the fluid velocity and $\boldsymbol{\sigma}_f$ is the dynamical stress tensor in the fluid domain defined by the constitutive relation

$$\boldsymbol{\sigma}_f = -p_f \mathbf{I} + \eta_f (\nabla \mathbf{v} + \nabla \mathbf{v}^\top), \quad (2.3)$$

where p_f is the pressure and η_f is the viscosity of the fluid. We assume the sphere is translating with velocity \mathbf{U} thus the no slip boundary condition dictates $\mathbf{v} = \mathbf{U}$ at the fluid-solid interface. In the reference configuration, the equilibrium momentum balance in the solid domain (Ω_s) yields

$$\nabla \cdot \boldsymbol{\sigma}_s + \mathbf{f}(t) = \mathbf{0}, \quad (2.4)$$

where $\boldsymbol{\sigma}_s$ is the solid elastic stress and \mathbf{f} is a body force density on the sphere. Since the motion is axisymmetric, we assume the elastic sphere reaches a stable equilibrium, wherein the velocity gradient field in the solid domain is zero and the sphere has a rigid motion thereafter [32, 33]. The constitutive relation for an isotropic incompressible neo-Hookean solid then can be expressed in terms of displacement vector \mathbf{u} [34, 35]

$$\boldsymbol{\sigma}_s = -p_s \mathbf{I} + \eta_s (\mathbf{F} \cdot \mathbf{F}^\top - \mathbf{I}), \quad (2.5)$$

where $\mathbf{F} = \mathbf{I} + \nabla \mathbf{u}$ is the deformation gradient tensor and η_s is the shear modulus. Here, p_s serves only as a Lagrange multiplier to impose the incompressibility of the solid through

$$\det(\mathbf{F}) = 1, \quad (2.6)$$

where $\det(\mathbf{F})$ is the determinant of tensor \mathbf{F} . The solid and fluid momentum balances are coupled through the continuity of normal traction at the interface $(\partial\Omega)$, which dictates

$$\boldsymbol{\sigma}_s \cdot \mathbf{n} = \boldsymbol{\sigma}_f \cdot \mathbf{n}, \quad (2.7)$$

where \mathbf{n} is the normal vector to the surface of the deformed sphere.

Without any loss of generality, we will assume that the translational velocity, $\mathbf{U} = U \mathbf{e}_z$, and the body force density, $\mathbf{f} = b f(t) \mathbf{e}_z$, are oriented along \mathbf{e}_z . For simplicity we assume a spatially uniform body force where b is a positive constant denoting the magnitude of the forcing while f is a dimensionless $O(1)$ function such that the elastic deformation may be considered quasistatic. Before going further, we non-dimensionalize all the equations defining dimensionless quantities $\hat{\nabla} = R_0 \nabla$, $\hat{\mathbf{u}} = \mathbf{u}/R_0$, $\hat{\mathbf{v}} = \mathbf{v}/U_{ch}$, $\hat{\mathbf{U}} = \mathbf{U}/U_{ch}$, $\hat{t} = t/(R_0/U_{ch})$, $\hat{p}_f = p_f/(\eta_f U_{ch}/R_0)$, $\hat{\boldsymbol{\sigma}}_f = \boldsymbol{\sigma}_f/(\eta_f U_{ch}/R_0)$, $\hat{\boldsymbol{\sigma}}_s = \boldsymbol{\sigma}_s/\eta_s$, $\hat{p}_s = p_s/\eta_s$ and $\hat{\mathbf{f}}(t) = \mathbf{f}(t)/(\eta_s/R_0)$, where $U_{ch} = 2bR_0^2/9\eta_f$. Here U_{ch} simply denotes the translational speed of a rigid sphere under a constant body force of magnitude b . Furthermore, for a forcing profile with frequency ω , we define $\nu = \omega R_0/U_{ch}$ as a ratio of time scales. Now for convenience, we drop the $(\hat{\cdot})$ notation

and henceforth refer to dimensionless variables. The dimensionless form of the boundary condition at the fluid-solid interface is then derived

$$\boldsymbol{\sigma}_s \cdot \mathbf{n} = \epsilon \boldsymbol{\sigma}_f \cdot \mathbf{n}, \quad (2.8)$$

where $\boldsymbol{\sigma}_f = -p_f \mathbf{I} + \nabla \mathbf{v} + \nabla \mathbf{v}^\top$ is the dimensionless stress in the fluid, $\boldsymbol{\sigma}_s = -p_s \mathbf{I} + \nabla \mathbf{u} + \nabla \mathbf{u}^\top + \nabla \mathbf{u} \cdot \nabla \mathbf{u}^\top$ is the dimensionless stress in the solid phase and $\epsilon = \eta_f U_{ch}/\eta_s R_0$ represents the ratio of the viscous forces to the elastic forces. In order to develop a geometric relation between the displacement vector and the surface deformations, we consider a spherical coordinate system (r, θ, ϕ) in the reference configuration. Since the motion is axisymmetric, we can define the surface as $r_s(\theta)$ where θ is the polar angle. For any material point, the displacement vector is defined $\mathbf{u} = \chi(\mathbf{X}, t) - \mathbf{X}$, where \mathbf{X} is the position vector in the reference configuration and $\chi(\mathbf{X}, t)$ is the deformation vector mapping each material point to its new location [34]. Thus, at the interface, this definition yields

$$\|\mathbf{X} + \mathbf{u}\| = r_s, \quad (2.9)$$

providing a geometric relation between surface equation and the displacement vector. It is important to note that the governing equations in Ω_s are expressed in the reference configuration. Thus, in enforcing the interface boundary condition given in equation (2.8), we shift the coordinate system accordingly and report our results in the spatial configuration.

A. Asymptotic analysis

Here we focus on the case wherein the elastic forces are much larger than the viscous forces, i.e., $\epsilon \ll 1$. We expand all the parameters in terms of ϵ and refer to the i^{th} order of any parameter using superscript (i) (e.g., $p_f = p_f^{(0)} + \epsilon p_f^{(1)} + \epsilon^2 p_f^{(2)} + \dots$). Due to the linearity of the Stokes equations, at any order the flow field around the sphere is governed by

$$-\nabla p_f^{(i)} + \nabla^2 \mathbf{v}^{(i)} = \mathbf{0}, \quad (2.10)$$

$$\nabla \cdot \mathbf{v}^{(i)} = 0, \quad (2.11)$$

where $\boldsymbol{\sigma}_f^{(i)} = -p_f^{(i)} \mathbf{I} + \nabla \mathbf{v}^{(i)} + \nabla \mathbf{v}^{(i)\top}$ and $i \in \{0, 1, 2, \dots\}$. We use the general solution given by Sampson for axisymmetric Stokes flow in the spherical coordinate system [1, 36]. The boundary conditions in the fluid domain thereby are $\mathbf{v}^{(i)} = 0$ at $r \rightarrow \infty$ and $\mathbf{v} = U \mathbf{e}_z$ at $r = r_s$. In the solid domain, the nonlinear governing equations are linearized perturbatively, thus we treat the problem at each order separately. As one can notice from equation (2.8), there is no deformation at the zeroth order thus the leading-order elastic effects are of $O(\epsilon)$.

1. Zeroth order flow field (first order solid deformations)

At zeroth order in the fluid domain, the motion is simply the translation of a rigid sphere in Stokes flow. Satisfying $\mathbf{v}^{(0)} = f \mathbf{e}_z$ at $r = 1$, we find

$$v_r^{(0)} = \frac{f}{2} \left(\frac{3}{r} - \frac{1}{r^3} \right) \cos \theta, \quad (2.12)$$

$$v_\theta^{(0)} = -\frac{f}{4} \left(\frac{3}{r} + \frac{1}{r^3} \right) \sin \theta, \quad (2.13)$$

$$p_f^{(0)} = \frac{3f}{2r^2} \cos \theta. \quad (2.14)$$

The leading-order deformation equations in the solid domain are in the form of the Stokes equations as

$$-\nabla p_s^{(1)} + \nabla^2 \mathbf{u}^{(1)} + \mathbf{f}(t) = \mathbf{0}, \quad (2.15)$$

$$\nabla \cdot \mathbf{u}^{(1)} = 0, \quad (2.16)$$

$$\boldsymbol{\sigma}_s^{(1)} = -p_s^{(1)} \mathbf{I} + \nabla \mathbf{u}^{(1)} + \nabla \mathbf{u}^{(1)\top}. \quad (2.17)$$

Thus, here as well, we can employ Sampson's general solution for an axisymmetric Stokes flow. At this order, the interface boundary condition is $\sigma_{s,rr}^{(1)} = \sigma_{f,rr}^{(0)}$ and $\sigma_{s,r\theta}^{(1)} = \sigma_{f,r\theta}^{(0)}$. Thus, we obtain

$$u_r^{(1)} = \frac{f}{2}(1 - r^2) \cos \theta, \quad (2.18)$$

$$u_\theta^{(1)} = \frac{f}{2}(-1 + 2r^2) \sin \theta, \quad (2.19)$$

$$p_s^{(1)} = -\frac{f}{2}r \cos \theta. \quad (2.20)$$

To find the surface deformation, we define surface equation $r_s = 1 + s(\theta)$ and use the geometric relation in (2.9), which at this order leads to $s^{(1)} = u_r^{(1)}$ at $r = 1$. Therefore, we find $s^{(1)} = 0$, indicating that the elastic sphere remains spherical with no surface deformation. We note that this result is similar to the sedimentation of a falling drop in a viscous fluid. Taylor and Acrivos [37] showed that when inertia is neglected and the flow fields both inside and outside the drop are similarly governed by the Stokes equations, the shape has to remain spherical to satisfy the continuity of the normal tractions at the interface.

2. First order flow field (second order solid deformations)

At this order, the flow field at surface of the sphere satisfies $\mathbf{v}^{(1)} = U^{(1)}\mathbf{e}_z$. Recalling that $s^{(1)} = 0$, we find

$$v_r^{(1)} = \frac{U_1 f^2}{2} \left(\frac{3}{r} - \frac{1}{r^3} \right) \cos \theta, \quad (2.21)$$

$$v_\theta^{(1)} = -\frac{U_1 f^2}{4} \left(\frac{3}{r} + \frac{1}{r^3} \right) \sin \theta, \quad (2.22)$$

$$p_f^{(1)} = \frac{3U_1 f^2 \cos \theta}{2r^2}, \quad (2.23)$$

where the first correction for translational velocity U_1 shall be determined by satisfying the interface boundary condition. In the solid domain, the governing equations are given by

$$-\nabla p_s^{(2)} + \nabla^2 \mathbf{u}^{(2)} + \nabla \left(\nabla \cdot \mathbf{u}^{(2)} \right) + \nabla \cdot \left(\nabla \mathbf{u}^{(1)} \cdot \nabla \mathbf{u}^{(1)\top} \right) = \mathbf{0}, \quad (2.24)$$

$$\nabla \cdot \mathbf{u}^{(2)} + \text{tr}(\nabla \mathbf{u}^{(1),c}) = 0, \quad (2.25)$$

where $\text{tr}(\cdot)$ and $(\cdot)^c$ indicate trace and cofactor of the tensor, respectively. Here the stress in the solid phase is defined

$$\boldsymbol{\sigma}_s^{(2)} = -p_s^{(2)} \mathbf{I} + \nabla \mathbf{u}^{(2)} + \nabla \mathbf{u}^{(2)\top} + \nabla \mathbf{u}^{(1)} \cdot \nabla \mathbf{u}^{(1)\top}. \quad (2.26)$$

Now, by enforcing the interface boundary conditions $\sigma_{s,rr}^{(2)} = \sigma_{f,rr}^{(1)}$ and $\sigma_{s,r\theta}^{(2)} = \sigma_{f,r\theta}^{(1)}$ at $r = 1$, we find $U_1 = 0$ and

$$u_r^{(2)} = -\frac{f^2 r}{304} (23 + 27r^2 + (69 + 5r^2) \cos 2\theta), \quad (2.27)$$

$$u_\theta^{(2)} = \frac{f^2 r}{304} (69 + 97r^2) \sin 2\theta, \quad (2.28)$$

$$p_s^{(2)} = \frac{f^2}{152} (190 - 199r^2 - 27r^2 \cos 2\theta), \quad (2.29)$$

leading to $p_f^{(1)} = 0$, $v_r^{(1)} = 0$ and $v_\theta^{(1)} = 0$. It is worthwhile to emphasize that the leading order corrections for the flow field (i.e., $v_r^{(1)}$ and $v_\theta^{(1)}$) are imposed by the leading order surface deformation in the solid domain. Thus, $s^{(1)} = 0$ indeed causes no disturbance in the flow field at this order. Finally, to find $s^{(2)}$, we use the geometric relation

$$s^{(2)} = u_r^{(2)} + \frac{(u_\theta^{(1)})^2}{2}, \quad \text{at } r = 1, \quad (2.30)$$

leading to $s^{(2)} = -\frac{31f^2}{304}(1 + 3 \cos 2\theta)$, which indicates a shape deviation from a sphere to an oblate spheroid of aspect ratio $1 - \frac{93}{152}f^2\epsilon^2$.

3. Second order flow field (third order solid deformations)

The no slip boundary condition for the Stokes equations at this order is $\mathbf{v}^{(2)} + s^{(2)} \frac{\partial \mathbf{v}^{(0)}}{\partial r} = U^{(2)} \mathbf{e}_z$. The second order flow field around the sphere is

$$v_r^{(2)} = \frac{U_2 f^3 \cos \theta}{2} \left(\frac{3}{r} - \frac{1}{r^3} \right) + \frac{93 f^3 \cos \theta}{1520} \left(\frac{2}{r} + \frac{1 - 15 \cos 2\theta}{r^3} - \frac{3 - 15 \cos 2\theta}{r^5} \right), \quad (2.31)$$

$$v_\theta^{(2)} = -\frac{U_2 f^3 \sin \theta}{4} \left(\frac{3}{r} + \frac{1}{r^3} \right) - \frac{93 f^3 \sin \theta}{6080} \left(\frac{4}{r} + \frac{13 + 15 \cos 2\theta}{r^3} - \frac{27 + 45 \cos 2\theta}{r^5} \right), \quad (2.32)$$

$$p_f^{(2)} = \frac{3U_2 f^3 \cos \theta}{2r^2} - \frac{93 f^3 \cos \theta}{3040} \left(\frac{4}{r^2} + \frac{15 - 75 \cos 2\theta}{r^4} \right). \quad (2.33)$$

Similar to the previous order, to determine the correction for the translational velocity (i.e., U_2), we need to solve the solid deformation equations at the third order given by

$$-\nabla p_s^{(3)} + \nabla^2 \mathbf{u}^{(3)} + \nabla \cdot (\nabla \cdot \mathbf{u}^{(3)}) + \nabla \cdot (\nabla \mathbf{u}^{(1)} \cdot \nabla \mathbf{u}^{(2)\top} + \nabla \mathbf{u}^{(2)} \cdot \nabla \mathbf{u}^{(1)\top}) = \mathbf{0}, \quad (2.34)$$

$$\nabla \cdot \mathbf{u}^{(3)} + \det(\nabla \mathbf{u}^{(1)}) + T = 0, \quad (2.35)$$

where T is the $O(\epsilon^3)$ contribution of $\text{tr}(\nabla \mathbf{u}^c)$. Here, the stress inside the solid is defined

$$\sigma_s^{(3)} = -p_s^{(3)} \mathbf{I} + \nabla \mathbf{u}^{(3)} + \nabla \mathbf{u}^{(3)\top} + \nabla \mathbf{u}^{(1)} \cdot \nabla \mathbf{u}^{(2)\top} + \nabla \mathbf{u}^{(2)} \cdot \nabla \mathbf{u}^{(1)\top}. \quad (2.36)$$

Enforcing the third order interface boundary conditions at $r = 1$ as

$$\sigma_{s,rr}^{(3)} + s^{(2)} \frac{\partial \sigma_{s,rr}^{(1)}}{\partial r} - \frac{ds^{(2)}}{d\theta} \sigma_{s,r\theta}^{(1)} = \sigma_{f,rr}^{(2)} + s^{(2)} \frac{\partial \sigma_{f,rr}^{(0)}}{\partial r} - \frac{ds^{(2)}}{d\theta} \sigma_{f,r\theta}^{(0)}, \quad (2.37)$$

$$\sigma_{s,r\theta}^{(3)} + s^{(2)} \frac{\partial \sigma_{s,r\theta}^{(1)}}{\partial r} - \frac{ds^{(2)}}{d\theta} \sigma_{s,\theta\theta}^{(1)} = \sigma_{f,r\theta}^{(2)} + s^{(2)} \frac{\partial \sigma_{f,r\theta}^{(0)}}{\partial r} - \frac{ds^{(2)}}{d\theta} \sigma_{f,\theta\theta}^{(0)}, \quad (2.38)$$

we finally find $U_2 = -\frac{31f^3}{380}$, and

$$u_r^{(3)} = (7r^2 (310r^2 - 2091) \cos 2\theta - 5816r^4 + 9645r^2 - 30240) \frac{f^3 \cos \theta}{25536}, \quad (2.39)$$

$$u_\theta^{(3)} = (7r^2 (434r^2 + 697) \cos 2\theta + 5284r^4 + 381r^2 + 10080) \frac{f^3 \sin \theta}{8512}, \quad (2.40)$$

$$p_s^{(3)} = -r (322r^2 \cos 2\theta + 3766r^2 - 2991) \frac{f^3 \cos \theta}{1596}. \quad (2.41)$$

Thence, we can determine the third order shape deformation using the geometric relation (2.9), which reads $s^{(3)} = u_r^{(3)} + u_\theta^{(1)} u_\theta^{(2)}$ at $r = 1$. Notably, we find $s^{(3)} = -\frac{2777f^3}{1824} \cos^3 \theta$ indicating a ‘egg-like’ deformation which exhibits a front-back asymmetry in the surface of the elastic sphere as shown in figure 1. To recover the solution for the case of translation under a constant body force (i.e. sedimentation), one can set $f = 1$. Then $U = 1 - \frac{31}{380} \epsilon^2 + O(\epsilon^3)$ suggesting a slower translational velocity, which is notably unlike the settling speed of a compressible Hookean sphere [31]. It is also worthwhile to note that elastic capsules containing viscous fluids exhibit a similar asymmetry in their deformation under pure translation. In a numerical study, Ishikawa *et al.* [38] showed that at steady state, a weakly-elastic spherical micro-torque swimmer deforms to an egg-like shape. A similar deformation was observed experimentally for sedimenting vesicles as well [32].

4. Third order flow field

To quantify the effect of the shape asymmetry on the motion of the particle, we shall determine the third order correction for the flow field. Once again, we solve the Stokes equations, but this time with $\mathbf{v}^{(3)} + s^{(3)} \frac{\partial \mathbf{v}^{(0)}}{\partial r} = U^{(3)} \mathbf{e}_z$ at $r = 1$. Thus, we can find the third order correction for the fluid field and stress field in terms of the translational velocity $U^{(3)}$. Now to find $U^{(3)}$, instead of solving for the next order solid deformation (as we did in the previous

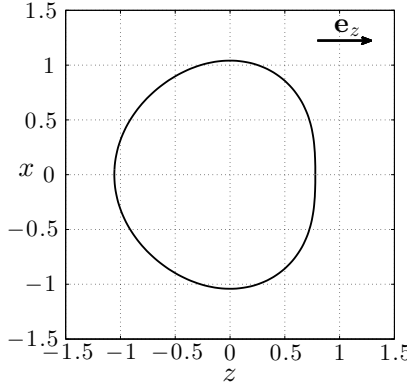


FIG. 1. Deformed shape of the translating elastic sphere when $f = 1$ and $\epsilon = 0.45$.

orders), we employ an auxiliary case wherein a rigid sphere of the same radius is translating with the same driving force [39]. For the elastic sphere, in the fluid domain, the driving force is balanced completely by surface forces

$$\mathbf{F}^{\text{dr}} + 3\epsilon \int_{\partial\Omega} \boldsymbol{\sigma}_f \cdot \mathbf{n} dS = \mathbf{0}, \quad (2.42)$$

where $\mathbf{F}^{\text{dr}} = \mathbf{f}V$ is the total driving force on the sphere, V is the volume and S represent dimensionless area element of the sphere. On the other hand, for the rigid sphere case, the drag law dictates $\mathbf{F}^{\text{dr}}/V = \frac{9f}{2}\epsilon \mathbf{e}_z$, thus

$$\frac{1}{V} \int_{\partial\Omega} \boldsymbol{\sigma}_f \cdot \mathbf{n} dS = -\frac{3f}{2} \mathbf{e}_z. \quad (2.43)$$

Now by substituting $\boldsymbol{\sigma}_f = \boldsymbol{\sigma}_f^{(0)} + \epsilon \boldsymbol{\sigma}_f^{(1)} + \epsilon^2 \boldsymbol{\sigma}_f^{(2)} + \epsilon^3 \boldsymbol{\sigma}_f^{(3)}$, we determine the left-side of equation (2.43) as $\frac{1}{V} \int_{\partial\Omega} \boldsymbol{\sigma}_f \cdot \mathbf{n} dS = -\frac{3}{2} (f + U^{(3)}\epsilon^3) \mathbf{e}_z$, indicating that $U^{(3)} = 0$. Thus, the final expression for the translational velocity

$$U = \left[1 - \frac{31}{380} f^2 \epsilon^2 + O(\epsilon^4) \right] f, \quad (2.44)$$

and the third order corrections in the flow field are

$$v_r^{(3)} = \frac{2777f^4}{17024} \left(\frac{1}{r^2} - \frac{1}{r^4} \right) \left(3 - 9 \cos^2 \theta - \frac{3 - 30 \cos^2 \theta + 35 \cos^4 \theta}{r^2} \right), \quad (2.45)$$

$$v_\theta^{(3)} = \frac{2777f^4}{34048} \left(\frac{\sin 2\theta}{r^4} \right) \left(12 - 14 \cos^2 \theta - \frac{12 - 28 \cos^2 \theta}{r^2} \right), \quad (2.46)$$

$$p_f^{(3)} = \frac{2777f^4}{42560} \left(\frac{1}{r^4} \right) \left(15 - 45 \cos^2 \theta - \frac{21 - 210 \cos^2 \theta + 245 \cos^4 \theta}{r^2} \right). \quad (2.47)$$

3. TWO-SPHERE SWIMMER

We consider a model swimmer which consists of two spheres: a rigid sphere A and a neo-Hookean isotropic incompressible elastic sphere B (identical to the elastic sphere defined in section 2). The spheres are of equal radii and linked by a rod of length L . To propel itself forward, the swimmer repeats a two-step, one-dimensional motion in which the connecting rod shortens its length in step (I), and then returns back to its original shape in step (II) (see figure 2). While advancing from one step to another, sphere B changes its shape instantaneously and then recovers the spherical shape again, once the step is completed. We note that despite the reversible actuation, the flow field induced by sphere B is not front-back symmetric. Thus, for sphere A, the contribution of the background flow (induced by sphere B) is different between step (I) and (II). The net motion in each cycle thereby is not kinematically reversible and indeed the swimmer can propel with a velocity that we determine below.

The connecting rod exerts driving forces \mathbf{F}_A and \mathbf{F}_B on spheres A and B, respectively. The force-free motion of the swimmer necessitates $\mathbf{F}_A + \mathbf{F}_B = \mathbf{0}$. To be able to use the results of section 2, we further simplify the model by

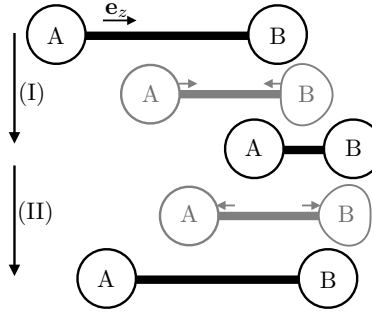


FIG. 2. One cycle of the two-step motion of the swimmer. Step (I): The rod shortens its length. Step (II): Spheres move away from one another until they reach the initial distance. The steps in grey colour demonstrate the swimmer while it proceeds to the next step and sphere B is deformed.

considering a spatially uniform force density for both spheres. Thus, the periodic motion illustrated in figure 2 can be imposed by prescribing $\mathbf{F}_A/V = -\mathbf{F}_B/V = \frac{9}{2}\epsilon \sin(\nu t)\mathbf{e}_z$. Assuming that spheres are well separated at all times, we employ a far-field approximation to determine the flow field around the swimmer. The velocity of each sphere, i.e. \mathbf{U}_A and \mathbf{U}_B , then follows the drag law

$$\mathbf{U}_A = \mathbf{R}_A^{-1} \cdot \mathbf{F}_A + \mathcal{F}_A [\mathbf{v}_{B \rightarrow A}], \quad (3.1)$$

$$\mathbf{U}_B = \mathbf{R}_B^{-1} \cdot \mathbf{F}_B + \mathcal{F}_B [\mathbf{v}_{A \rightarrow B}], \quad (3.2)$$

where \mathbf{R}_A and \mathbf{R}_B are hydrodynamic resistance tensors for spheres A and B, \mathcal{F}_A and \mathcal{F}_B are the Faxèn operators, and $\mathbf{v}_{B \rightarrow A}$ ($\mathbf{v}_{A \rightarrow B}$) is the background flow field on sphere A (B), induced by sphere B (A). Here, to focus only on the leading order propulsion velocity, we limit our calculations to the first reflection of the flow fields. Therefore, we neglect the contribution of the background flow on the deformation of sphere B. Here we also employ a quasistatic assumption for the elastic deformations and thus consider that sphere B changes its shape instantly in response to variations in the forcing. At each step, we take the average velocity of the two spheres as the instantaneous velocity of the swimmer, defining $\mathbf{U}^{(I)} = \frac{\mathbf{U}_A^{(I)} + \mathbf{U}_B^{(I)}}{2}$ and $\mathbf{U}^{(II)} = \frac{\mathbf{U}_A^{(II)} + \mathbf{U}_B^{(II)}}{2}$, where superscripts (I) and (II) refer to the quantities at the corresponding steps. Thence, to find the net propulsion velocity we average the swimming velocities over one complete cycle

$$\bar{\mathbf{U}} = \frac{1}{\tau} \left(\int_0^{\tau/2} \mathbf{U}^{(I)} dt + \int_{\tau/2}^{\tau} \mathbf{U}^{(II)} dt \right), \quad (3.3)$$

where $\tau = 2\pi/\nu$ is the period of the cycle. By making use of equations (3.1) and (3.2) and noting that $\mathbf{F}_A(t + \frac{\tau}{2}) = -\mathbf{F}_A(t)$ and $\mathbf{F}_B(t + \frac{\tau}{2}) = -\mathbf{F}_B(t)$, equation (3.3) can be reduced to

$$\bar{\mathbf{U}} = \frac{1}{2\tau} \left\{ \int_0^{\tau/2} \left(\mathcal{F}_A [\mathbf{v}_{B \rightarrow A}^{(I)}] + \mathcal{F}_B [\mathbf{v}_{A \rightarrow B}^{(I)}] \right) dt + \int_{\tau/2}^{\tau} \left(\mathcal{F}_A [\mathbf{v}_{B \rightarrow A}^{(II)}] + \mathcal{F}_B [\mathbf{v}_{A \rightarrow B}^{(II)}] \right) dt \right\}. \quad (3.4)$$

From the general description of Faxèn operator [40, 41], we find $\mathcal{F}_A = 1 + \frac{1}{6}\nabla^2$ and $\mathcal{F}_B = 1 + \left(\frac{1}{6} + \frac{31}{228}\epsilon^2\right)\nabla^2 + O(\epsilon^3/l^2)$. Now using the asymptotic descriptions of the flow fields reported in section 2, we arrive at the leading order propulsion velocity

$$\bar{\mathbf{U}} = \frac{24993}{136192} \frac{\epsilon^3}{L^2} \mathbf{e}_z. \quad (3.5)$$

We note that the deformation of the sphere governs the propulsive thrust and that the magnitude of the change in distance between the spheres does not contribute to the leading order motion, unlike the three sphere swimmer where the difference in arm lengths quantifies the asymmetry [15].

4. CONCLUSION

In this paper, we inquired about the effects of elasticity on swimming in Stokes flow. We started by addressing the pure translation of an elastic particle in viscous fluid. We asymptotically showed that under a body force the

translational velocity of an elastic sphere is slower, and also the shape deformation is not front-back symmetric. The latter indicates an asymmetry in the surrounding flow field which can be exploited to evade the scallop theorem. To highlight the effect of this shape deformation on swimming, we proposed a very simple swimmer of two spheres that can swim with a reversible actuation, solely due to elasticity of one of the spheres. Our results show that accounting for elasticity of bodies may be crucial to fully understand the dynamics of swimming cells and specifically can be useful in designing microswimmers. Finally we note that while conceptually simple, our elastic two-sphere swimmer is not very effective for small deformations, but in practice one might use an elastic body which is already asymmetric to exacerbate this effect.

ACKNOWLEDGMENTS

The authors thank Professor G. M. Homsy for helpful discussions and support to B.N. through NSERC Grant No. RGPIN-386202-10. G.J.E. acknowledges funding from the NSERC Grant No. RGPIN-2014-06577.

[1] J. Happel and H. Brenner, *Low Reynolds Number Hydrodynamics* (Springer Netherlands, 1981).

[2] S. Kim and J. S. Karilla, *Microhydrodynamics: principles and selected applications* (Butterworth-Heinemann, 1991).

[3] A. J. Roberts, T. Kon, P. J. Knight, K. Sutoh, and S. A. Burgess, *Nat. Rev. Mol. Cell Biol.* **14**, 713 (2013).

[4] E. M. Purcell, *Am. J. Phys.* **45**, 3 (1977).

[5] E. Lauga, *Soft Matter* **7**, 3060 (2011).

[6] R. Trouilloud, T. S. Yu, A. E. Hosoi, and E. Lauga, *Phys. Rev. Lett.* **101**, 048102 (2008).

[7] E. Lauga, *EPL* **86**, 64001 (2009).

[8] D. Gonzalez-Rodriguez and E. Lauga, *J. Phys. Condens. Matter* **21**, 204103 (2009).

[9] J. Lighthill, *Mathematical Biofluidynamics* (SIAM, 1975).

[10] E. Lauga and T. R. Powers, *Rep. Prog. Phys.* **72**, 096601 (2009).

[11] R. Dreyfus, J. Baudry, and H. A. Stone, *EPJ B* **47**, 161 (2005).

[12] M. Iima and A. S. Mikhailov, *EPL* **85**, 44001 (2009).

[13] R. Golestanian, *Phys. Rev. Lett.* **105**, 018103 (2010).

[14] A. Najafi and R. Zargar, *Phys. Rev. E* **81**, 067301 (2010).

[15] A. Najafi and R. Golestanian, *Phys. Rev. E* **69**, 062901 (2004).

[16] R. Golestanian and A. Ajdari, *Phys. Rev. E* **77**, 036308 (2008).

[17] M. Leoni, J. Kotar, B. Bassetti, P. Cicuta, and M. Cosentino Lagomarsino, *Soft Matter* **2**, 472 (2009).

[18] J. E. Avron, O. Kenneth, and D. H. Oaknin, *New J. Phys.* **7**, 234 (2005).

[19] C. H. Wiggins and R. E. Goldstein, *Phys. Rev. Lett.* **80**, 3879 (1998).

[20] M. C. Lagomarsino, F. Capuani, and C. P. Lowe, *J. Theor. Biol.* **224**, 215 (2003).

[21] G. J. Elfring and E. Lauga, *J. Fluid Mech.* **674**, 163 (2011).

[22] R. E. Goldstein, E. Lauga, A. I. Pesci, and M. R. E. Proctor, *Phys. Rev. Fluids* **1**, 073201 (2016).

[23] T. Niedermayer, B. Eckhardt, and P. Lenz, *Chaos* **18**, 037128 (2008).

[24] D. R. Brumley, M. Polin, T. J. Pedley, and R. E. Goldstein, *Phys. Rev. Lett.* **109**, 268102 (2012).

[25] B. Nasouri and G. J. Elfring, *Phys. Rev. E* **93**, 033111 (2016).

[26] K. Son, J. S. Guasto, and R. Stocker, *Nature Phys.* **9**, 494 (2013).

[27] M. K. Jawed, N. K. Khouri, F. Da, E. Grinspun, and P. M. Reis, *Phys. Rev. Lett.* **115**, 168101 (2015).

[28] L. Li, H. Manikantan, D. Saintillan, and S. E. Spagnolie, *J. Fluid. Mech.* **735**, 705 (2013).

[29] T. Gao, H. H. Howard, and P. Ponte Castañeda, *J. Fluid. Mech.* **687**, 209 (2011).

[30] V. Galstyan, O. S. Pak, and H. A. Stone, *Phys. Fluids* **27**, 032001 (2015).

[31] T. Murata, *J. Phys. Soc.* **48**, 1738 (1980).

[32] Z.-H. Huang, M. Abkarian, and A. Viallat, *New J. Phys.* **13**, 035026 (2011).

[33] M. M. Villone, F. Greco, M. Hulsen, and P. L. Maffettone, *J. Non-Newton Fluid.* **234**, 105 (2016).

[34] M. E. Gurtin, E. Fried, and A. Lallit, *The Mechanics and Thermodynamics of Continua* (Cambridge University Press, 2010).

[35] R. W. Ogden, *Non-linear elastic deformations* (Dover, 1984).

[36] R. A. Sampson, *Phil. Trans. R. Soc. Lond. A* **182**, 449 (1891).

[37] T. D. Taylor and A. Acrivos, *J. Fluid Mech.* **18**, 466 (1964).

[38] T. Ishikawa, T. Tanaka, Y. Imai, T. Omori, and D. Matsunaga, *Proc. R. Soc. A* **472**, 20150604 (2016).

[39] L. E. Payne and W. H. Pell, *J. Fluid Mech.* **7**, 529 (1960).

[40] H. Brenner, *Chem. Eng. Sci.* **19**, 703 (1964).

[41] S. Kim, *Int. J. Multiph. Flow* **11**, 713 (1985).